Supplemental Material

Superconductivity in single-crystalline, aluminum- and gallium-hyperdoped germanium

Slawomir Prucnal[1], Viton Heera[1], René Hübner[1], Mao Wang[1], Grzegorz P. Mazur[2,3], Michał J. Grzybowski[2,3], Xin Qin[4], Ye Yuan[1,5], Matthias Voelskow[1], Wolfgang Skorupa[1], Lars Rebohle[1], Manfred Helm[1], Maciej Sawicki[3], Shengqiang Zhou[1]

1. Helmholtz-Zentrum Dresden-Rossendorf, Institute of Ion Beam Physics and Materials Research, Bautzner Landstraße 400, D-01328 Dresden, Germany

2. Institute of Physics, Polish Academy of Sciences, Aleja Lotnikow 32/46, PL-02668 Warsaw, Poland

3. International Research Centre MagTop, Institute of Physics, Polish Academy of Sciences, Aleja Lotnikow 32/46, PL-02668 Warsaw, Poland

4. Hefei National Laboratory for Physical Sciences at the Microscale, University of Science and Technology of China, Hefei, Anhui, 230026, China.

5. Physical Science and Engineering Division, King Abdullah University of Science and Technology, 23955-6900 Thuwal, Saudi Arabia

2. Experimental

2.1. Sample fabrication

N-type (Sb-doped, $\rho > 10$ Ωcm), (100)-oriented Ge wafers are used as substrates for acceptor implantation in order to electrically isolate the processed layer from the substrate by the formation of a p-n junction. First, a 30 nm thick SiO_2 cover layer is sputter-deposited to protect the Ge surface during ion implantation and annealing. Then samples were implanted with Al and Ga ions. Al was implanted with two different fluences of 2 and 4×10^{16} cm^2 and an energy of 50 keV. Ga ions were implanted with three fluences of 1, 2 and 4×10^{16} cm^2 and an energy of 100 keV. After ion implantation, samples were treated by flash lamp annealing (FLA) using different annealing times (3, 6 and 20 ms) and energy densities deposited onto the sample surface (from 50 up to 130 Jcm^{-2}). We have also tested the front- and rear-side annealing.

According to our previous experiments for Ga-implanted Ge [1], front-side FLA leads to the formation of a polycrystalline layer. The same effect was observed for Al-implanted samples. After front FLA, the implanted layer consists of an about 30 nm thick polycrystalline layer and a 70 nm thick single-crystalline layer which is formed due to explosive solid phase epitaxy [2]. The influence of FLA on the recrystallization process of ion-implanted Ge is explained with details in Ref. 2. Therefore, we focused here on rear-side annealing only. In order to recrystallize the implanted layer, the energy deposited into the rear side must be transferred through the entire wafer to the front side. The thermal conductivity of Ge determines the minimum annealing time needed to recrystallize the implanted layer. The maximum energy density deposited onto the sample surface (peak temperature) is limited by the melting temperature. For a 400 μm thick Ge wafer, the optimum annealing time was found to be 20 ms, both for Al- and for Ga-implanted samples.

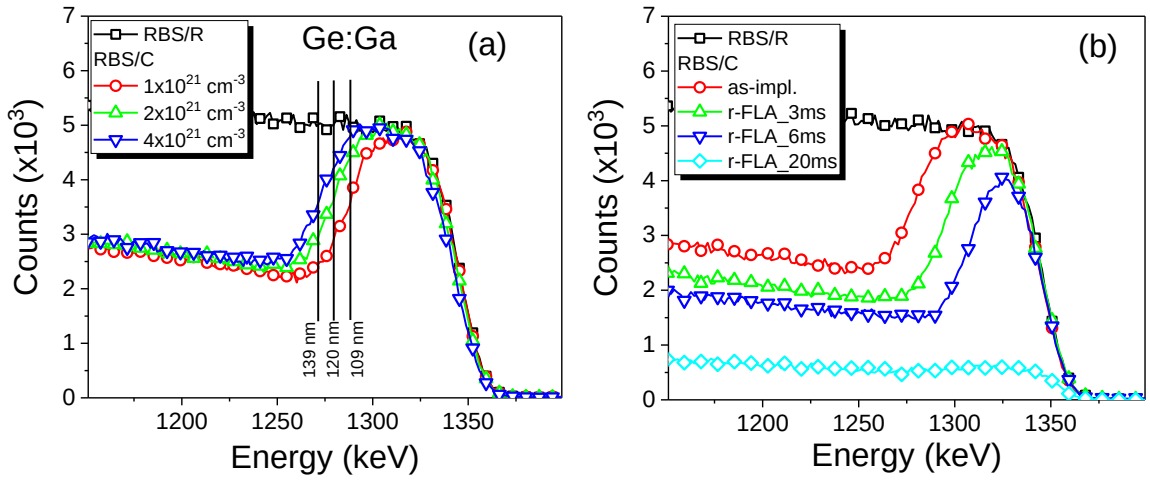

Figure S1. The RBS/R and RBS/C spectra obtained from Ga-hyperdoped Ge. (a) shows the RBS spectra obtained from the as-implanted samples with Ga concentrations at a level of 1, 2 and 4 × 10^{21} cm^{-3}, whereas the amorphous layer thicknesses are given for each case. (b) shows the influence of the pulse duration on the recrystallization of Ga-implanted Ge with a Ga concentration of 2 × 10^{21} cm^{-3}.

Figure S1a shows random (RBS/R) and channelling Rutherford backscattering (RBS/C) spectra obtained from as-implanted Ge samples containing three different Ga concentrations. The thicknesses of the amorphous layers for each Ga concentration is calculated based on the RBS data using the RUMP Software [3]. Later, these thicknesses were used to calculate the effective carrier concentration measured using the Hall Effect. The broadening of the amorphous layer with increasing Ga concentration is due to the high-fluence implantation process (elastic

scattering between already implanted and new ions). In the case of Al, we have used only two concentrations of 2 and 4×10^{21} cm^{-3}. The RBS data are similar to those presented in Fig. S1a. The Al-implanted Ge samples were annealed with conditions optimized for Ga-doped Ge, therefore, we expect a comparable evolution of the recrystallization process during FLA. Figure S1b shows the evolution of the explosive solid phase epitaxy as a function of annealing time. The melting point of Ge determines for each pulse length the maximum energy density which can be deposited onto the rear side of the implanted sample. For each annealing time, the flashed side was fully or partially molten. This means that the peak temperature at the flashed surface (rear side) reaches 938 ^{o}C. When the annealed surface becomes liquid, its optical reflectivity increases dramatically due to the strong increase of the amount of free equilibrium carriers in a molten crystal [4]. Therefore, using rear-side flash lamp or laser annealing, the temperature at the front side depends on the flash/laser parameters, thickness and thermal conductivity of the annealed material. As can be seen in Figure S1b, after FLA for 3 and 6 ms, only a part of the implanted Ge recrystallizes. The full recrystallization of the implanted layer appears after FLA for 20 ms. After annealing for 20 ms, the temperature at the implanted surface is in the range of 850 ^{o}C (see Fig. 1b in the main text). Importantly, the total heating/cooling process takes less than 100 ms. Using 3 ms pulse length, the temperature difference between the rear and front sides is above 250 K, while the explosive solid phase epitaxy takes place when the temperature of the annealed material is close to the melting point. Therefore, after 3 or 6 ms pulse length the implanted Ge layer started to recrystallize via conventional solid phase epitaxy which is to slow to recrystallize 120 nm within few milliseconds. In principle, the explosive solid phase epitaxy is possible also for short flash pulses (below 6 ms). In order to reduce the temperature gradient between the rear side and the front side, thinner wafers are needed.

The microstructural properties of the implanted and annealed samples were investigated by transmission electron microscopy (TEM). Figure S2 shows cross-sectional bright-field images obtained from Al- and Ga-hyperdoped Ge with the highest dopant concentration (4×10^{21} cm^{-3}) after FLA as well as the corresponding element distributions obtained by spectrum imaging analysis based on energy-dispersive X-ray spectroscopy (EDXS) in scanning TEM mode for a representative surface region of each sample, as marked by the gray squares in Fig. S2a and c. In both samples, the bright-field images reveal the presence of amorphous inclusions within the recrystallized Ge (Figs. S2a and c). High-resolution TEM images (not shown here) confirm this observation. In the case of the Al-implanted sample, the Al distribution within Ge agrees well with the spherically shaped amorphous inclusions. Additionally, a well-defined aluminum oxide layer is found at the Ge/SiO_2 interface (Fig. S2d). For the Ga-implanted sample, such

interface layer is not observed. Rather, most of the Ga is evenly distributed within the recrystallized Ge, while an additional fraction is segregated in spherical clusters (Fig. S2b). However, these Ga-rich clusters do not necessarily coincide with the irregularly shaped amorphous inclusions. .

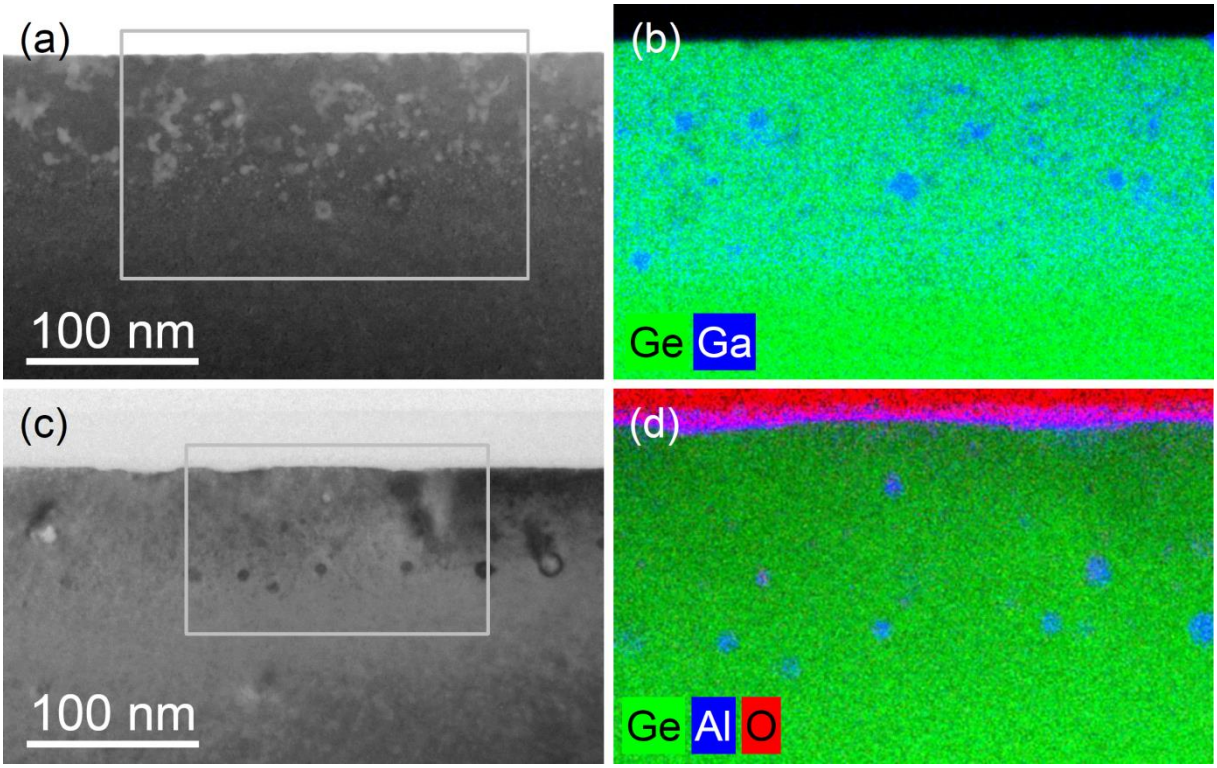

Figure S2. (a) and (c) Cross-sectional bright-field images obtained from Ga- and Al-hyperdoped Ge after FLA, respectively, (b) and (d) superimposed Ge (green), O (red) and Al or Ga (blue), respectively, element distributions obtained by spectrum imaging analysis based on EDXS in scanning TEM mode for a representative surface region of each sample, as marked by the squares in (a) and (c).

The aluminum oxide and SiO_2 capping layers were removed before electrical contact formation, which is why these oxides do not affect the electrical measurements. In summary, according to RBS and cross-sectional TEM investigation, we have determined that the maximum acceptor concentration which can be incorporated into the Ge crystal without cluster formation is in the range of 2×10^{21} cm^{-3}, both for Al and for Ga. Figure S3 shows the sheet resistance as a function of temperature for Al- and Ga-hyperdoped Ge with different dopant concentrations. For the lowest doping level, the investigated samples show a decrease of resistance down to 80 K,

followed by a slight increase up to 30 K and a stabilization for temperatures below 30 K. In the case of Ge samples containing 6 at.% of Al or more than 10 at.% of Ga, the sheet resistance continuously decreases with decreasing temperature.

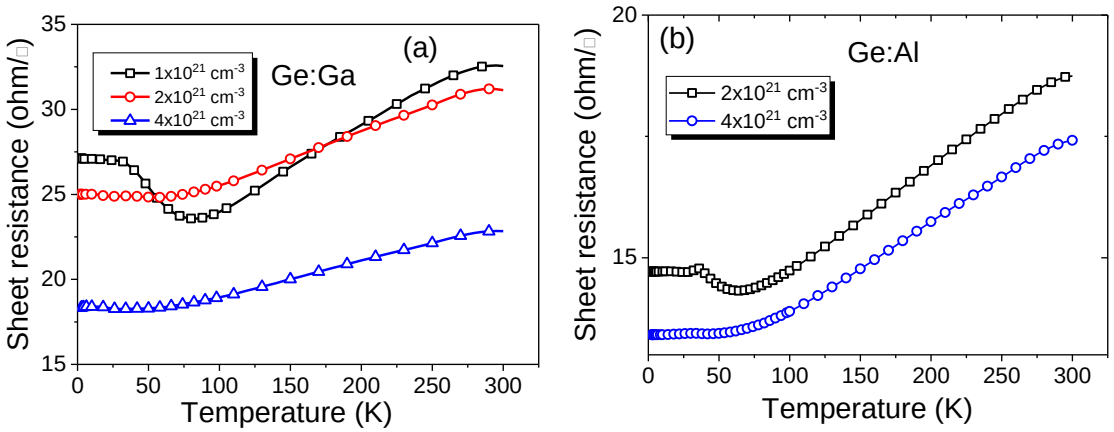

Figure S3. Sheet resistance as a function of temperature in the temperature range of 3 to 300 K for Ga (a) and Al (b) doped Ge after FLA for 20 ms with an energy density of 120 Jcm^{-2}.

The continuous decrease of sheet resistance with decreasing temperature is typical for metal-like samples. All samples with dopant concentration equal to or higher than 2×10^{21} cm^{-3} show superconductivity. The critical temperature (T_C) increases above 1 K with increasing acceptor concentration, but the effective carrier concentration doesn't increase significantly. Moreover, cross-sectional TEM reveals cluster formation for the samples with the highest dopant concentration. Hence, we concluded that the Ga-rich and Al-rich nanoprecipitates are responsible for the high-temperature superconductivity (T_C>1 K) in Ge.

References:

1. V. Heera, A. Mücklich, M. Posselt, M. Voelskow, C. Wündisch, B. Schmidt, R. Skrotzki, K. H. Heinig, T. Herrmannsdörfer, and W. Skorupa, Heavily Ga-doped germanium layers produced by ion implantation and flash lamp annealing: Structure and electrical activation, *J. Appl. Phys.* **107**, 053508 (2010).
2. S. Prucnal, F. Liu, M. Voelskow, L. Vines, L. Rebohle, D. Lang, Y. Berencén, S. Andric, R. Boettger, M. Helm M *et al.*, Ultra-doped n-type germanium thin films for sensing in the mid-infrared, *Sci. Rep.* **6**, 27643 (2016).
3. L. R. Doolittle, Algorithms for the rapid simulation of Rutherford backscattering spectra, *Nucl. Instr. and Meth.*, **9**, 344-351 (1985).

4. L. M. Blinov, V. S. Vavilov, G. L. Galkin, Changes in the optical properties and carrier density in silicon and gallium arsenide caused by strong photon-excitation with a ruby laser. Sov. Phys. Semicond. **1**, 1124 (1967)